Synthesis, structural study, and magnetic susceptibility of the chalcogenide olivine compound Mn_2SiTe_4 †

GERZON E. DELGADO[*1], *PILAR DELGADO-NIÑO*[2], *CECILIA CHACÓN*[3], *GUSTAVO MARROQUIN*[4], *IVÁN BRITO*[5].

1 Laboratorio de Cristalografía, Departamento de Química, Facultad de Ciencias, Universidad de Los Andes, Mérida 5101, Venezuela.
2 Facultad de Ingeniería Industrial, Universidad Distrital Francisco José de Caldas, Bogotá 111071, Colombia.
3 Conahcyt - Instituto Mexicano del Petróleo, Centro de Tecnologías para Exploración y Producción, Boca del Rio, Veracruz 94286, México.
4 Instituto Mexicano del Petróleo, Ciudad de México 07730, México.
5 Departamento de Química, Facultad de Ciencias Básicas, Universidad de Antofagasta, Antofagasta 1240000, Chile.

ABSTRACT

The ternary material Mn_2SiTe_4 was synthesized by direct fusion using the annealing method. X-ray powder diffraction analysis indicated that this material crystallizes in the olivine-type structure, space group Pnma, Z = 4, with unit cell parameters: a = 13.905(2) Å, b = 8.128(1) Å, c = 6.526(1) Å, V = 737.6(2) Å3. This olivine structure can be described from a hexagonal close-packing of selenium atoms where manganese atoms occupy ½ of the octahedral sites while silicon atoms lay in ⅛ of the tetrahedra. The magnetic susceptibility curve indicate a possible antiferromagnetic behavior for this material. This compound is related to the ternary layered $Mn_3Si_2Te_6$ recently studied as possible two-dimensional (2D) magnetic material.

Keywords: *olivines, chalcogenides, semiconductors, chemical synthesis, X-ray powder diffraction, Rietveld refinement, crystal structure, magnetic susceptibility.*

INTRODUCTION

Magnetic semiconducting materials have attractive properties and have received attention because of their potential application in optoelectronic and magnetic devices [1]. The materials more frequently studied are known as semimagnetic semiconductors, obtained from the tetrahedrally coordinated derivatives of the II-VI binaries [2]. One of these families is II_2-IV-VI_4, or more precisely II_2-IV-□-VI_4 where □ denotes the cation vacancy which is included to maintain the same number of cations and anions sites. These materials can be regarded as derived from the II-VI binaries, in which the cation has been substituted by two types of cations and an array of vacancies is introduced[2].

From the crystallographic point of view, three different structure has been reported for the II_2-IV-VI_4 family of compounds; a distorted spinel structure with tetragonal space group $I4_1/\alpha$ (N° 88) for Fe_2SnS_4[3], an orthorhombic structure with space group *Cmmm* (N° 65) for Mn_2SnS_4[4], and an orthorhombic structure with space group *Pnma* (N° 62) known as olivine-type, which comes from the crystal structure of the mineral Mg_2SiO_4[5].

It is important to mention that these materials generally crystallize in the olivine-type structure, as shown in Table 1 for Mn derivatives [6-12], with IV = Si, Ge, Sn, VI = S, Se, Te, where the VI anions forming a hexagonal close packing, and the cations in tetrahedral (IV) and octahedral (II) coordination. Particularly those olivine-type compounds containing transition metals are known as versatile magnetic materials13, have been considered as good model systems to study multi-critical phenomena [14], have found important new applications also for thermoelectric power generation15, and as cathode materials for batteries [16].

Concerning the ternary Mn_2SiTe_4, its crystal structure has not been established. A search in the databases Powder Diffraction File PDF-ICDD [21], Inorganic Crystal Structure Database (ICSD) [22], and Springer Materials [23] showed no entries for this chalcogenide compound. Recently, in a study about the prediction of A_2BX_4 metal-chalcogenide compounds via first-principles thermodynamics, the authors indicate that Mn_2SiTe_4

***Author for correspondence:** *gerzon@ula.ve*

† Dedicated to the memory of Professor Santos Adán López-Rivera

Table 1. Crystallography information for the Mn_2-IV-VI_4 (IV= Si, Ge, Sn; VI= S, Se, Te) system and Curie temperature (Θ) reported to date.

Ternary	SG	a (Å)	b (Å)	c (Å)	V (Å^3)	Ref.	Θ(K)	Ref.
Mn_2SiS_4	*Pnma*	12.688 (2)	7.429 (2)	5.942 (1)	560.1 (2)	[6]	-200	[17]
Mn_2SiS_4	*Pnma*	13.3066(8)	7.7780(5)	6.2451(3)	646.4(1)	[7]	-230	[7]
Mn_2SiTe_4	*Pnma*	13.905(2)	8.128(1)	6.526(1)	737.6(2)	this work	---	---
Mn_2GeS_4	*Pnma*	12.776	7.441	6.033	573.53	[8]	-373	[13]
Mn_2GeSe_4	*Pnma*	13.350(3)	7.765(2)	6.307(1)	635.8(3)	[9]	-240	[9]
Mn_2GeTe_4	*Pnma*	13.950(2)	8.115(1)	6.592(1)	746.2(2)	[10]	-375	[18]
Mn_2SnS_4	*Cmmm*	7.397(4)	10.477(7)	3.664(3)	284.0(1)	[4]	-463	[19]
Mn_2SnSe_4	*Pnma*	12.9028(2)	7.9001(1)	6.5015(1)	662.72(2)	[11]	-	
Mn_2SnTe_4	*Pnma*	14.020(2)	8.147(1)	6.607(1)	754.7(2)	[12]	-300	[20]

is predicted to be stable, between other 24 ternary tellurides unreported compounds, with a formation enthalpy of -0.36 eV/atom [24]. This compound is related to Mn_3Si2Te_6 recently studied as a possible two-dimensional (2D) magnetic material [25] with van der Waals (vdW) engineering of magnetism properties [26].

It is important to establish the crystal structure of semiconductor materials to understand and explain their physical properties. With the expectation of providing a complete description of the Mn_2SiTe_4 crystal structure, in the present work, and as part of the ongoing crystalline structural studies on ternary and quaternary chalcogenide compounds [27-36], we report the structural characterization of this ternary material using powder X-ray diffraction. The susceptibility curve for this material contributes to show some results on their magnetic properties.

EXPERIMENTAL SECTION

Synthesis

Polycrystalline sample of the ternary phase Mn_2SiTe_4 was synthesized by direct fusion of stoichiometric quantities of Mn, Si, and Te elements, with a nominal purity of at least 99.99% (Sigma-Aldrich), in a sealed, evacuated quartz ampoule, which was previously subject to pyrolysis to avoid reaction of the starting materials with quartz.

The fusion process, 14 days, was carried out into a furnace in a vertical position heated up to 1050°C. Then, the temperature was gradually lowered to 500°C. Finally, the furnace was turned off and the ingots were cooled to room temperature.

Chemical analysis

The chemical composition of the resultant ingot was determined at several regions by energy-dispersive X-ray (EDS) analysis using a JMS-6400 scanning electron microscope (SEM). Three different regions of the ingot were scanned, and the average atomic percentages are Mn (14.5%), Si (28.3%), and Te (57.2%), very close to the ideal composition 2:1:4. The error in the standardless analysis was around 5%.

X-ray powder diffraction

X-ray powder diffraction pattern was collected, at room temperature, in a Panalytical X'pert diffractometer with CuKα radiation (λ= 1.5418 Å). A small quantity of the sample was ground mechanically in an agate mortar and pestle and mounted on a flat holder covered with a thin layer of grease. The specimen was scanned from 10-100° 2□, with a step size of 0.02° and a counting time of 15s. Silicon (SRM-640) was used as an external standard. The Panaytical X'pert Pro analytical software was used to establish the positions of the peaks.

Magnetic susceptibility

Measurements of magnetic susceptibility χ as a function of temperature T in the range 2-300 K were made with a fixed value of magnetic field B of 100 G, using a Quantum Design SQUID magnetometer.

RESULTS AND DISCUSSION

The X-ray powder pattern of Mn_2SiTe_4 is shown in Figure 1, which indicates a single phase. The 20 first measured reflections were indexed using the program Dicvol04 [37], which gave a unique solution in an orthorhombic cell with parameters a = 13.891(2) Å, b = 8.113(1) Å, and c = 6.531(1) Å. Systematic absence analysis indicates a P-type cell, which suggested along with the sample composition and cell parameter dimensions that this material is isostructural with the olivine-type compounds, crystallizing in the orthorhombic space group *Pnma* (Nº62) with 4 molecules in the asymmetric unit (Z = 4).

The Rietveld refinement [38] of the whole diffraction pattern was carried out using the Fullprof program [39]. The atomic coordinates of the isomorphic compound Mn_2SnTe_4 [12] were

Table 2. Rietveld refinement results for Mn_2SiTe_4.

Chemical Formula	Mn_2SiTe_4	Data range 2□ (°)	10-100º
Formula weight (g/mol)	648.4	Step size 2□ (°)	0.02
Crystal system	Orthorhombic	Counting time (s)	15
Space group	Pnma (Nº 62)	N° step intensities	4501
a (Å)	13.905(2)	Peak-shape profile	Pseudo-Voigt
b (Å)	8.128(1)	Nº refined parameters	26
c (Å)	6.526(1)	Rp (%)	5.4
V (Å3)	737.6(2)	Rwp (%)	6.0
Z	4	Rexp (%)	5.1
Dcalc(g/cm3)	5.84	χ2	1.4
Temperature (K)	273(2)	S	1.2

$R_p = 100\ \Sigma|y_{obs} - y_{calc}| / \Sigma|_{yobs}|$ $R_{wp} = 100\ [\Sigma_w|y_{obs} - y_{calc}|^2 / \Sigma_w|y_{obs}|^2]^{1/2}$ $R_{exp} = 100\ [(N\text{-}P+C) / \Sigma_w(y_{obs}^2)]^{1/2}$ $\chi^2 = [R_{wp}^2 / R_{exp}^2]^{1/2}$

$S = R_{wp} / R_{exp}$ (goodness of fit) N-P+C is the number of degrees of freedom

used as the initial model for the refinement of Mn_2SiTe_4, with the unit cell parameters obtained in the indexing. The angular dependence of the peak full width at half maximum (FWHM) was described by Cagliotti's formula [40]. Peak shapes were described by the parameterized Thompson-Cox-Hastings pseudo-Voigt profile function [41].

The background was described by the automatic interpolation of 50 points throughout the whole pattern. The thermal motion of the atoms was described by one overall isotropic temperature factor. Details of the Rietveld refinement of Mn_2SiTe_4 are summarized in Table 2, and the atomic positions and thermal displacement factors are presented in Table 3. The observed, calculated, and residual powder XRD patterns of Mn_2SiTe_4 are shown in Figure 1.

Mn_2SiTe_4 crystallizes in an olivine-type structure. This olivine structure can be described as a hexagonal close packing of Te^{-2} anions with the Mn^{+2} cations occupying half of the octahedral sites and the Si^{+4} cations occupying an eighth of the tetrahedral sites. As expected for these materials each anion is coordinated by four cations (three Mn and one Si) located at the corners of a slightly distorted tetrahedron. The Mn_1Te_6 octahedra are located at a center of symmetry and form infinite edge-shared chains parallel to [010].

In alternating positions to the left and right of the chains and situated halfway between two Mn_1Te_6 octahedra, the Mn_2Te_6 octahedra are straddling the mirror planes perpendicular to [010]. The telluride anion common to the two octahedra Mn_1Te_6 and the Mn_2Te_6 octahedron forms one of the apices of an occupied $SiTe_4$ tetrahedron; the other 3 apices are located in a horizontal plane and are provided by 3 telluride anions of the

Figure 1. Observed (·), calculated (-), and difference plot of the final Rietveld refinement of Mn_2SiTe_4. The Bragg reflections are indicated by vertical bars.

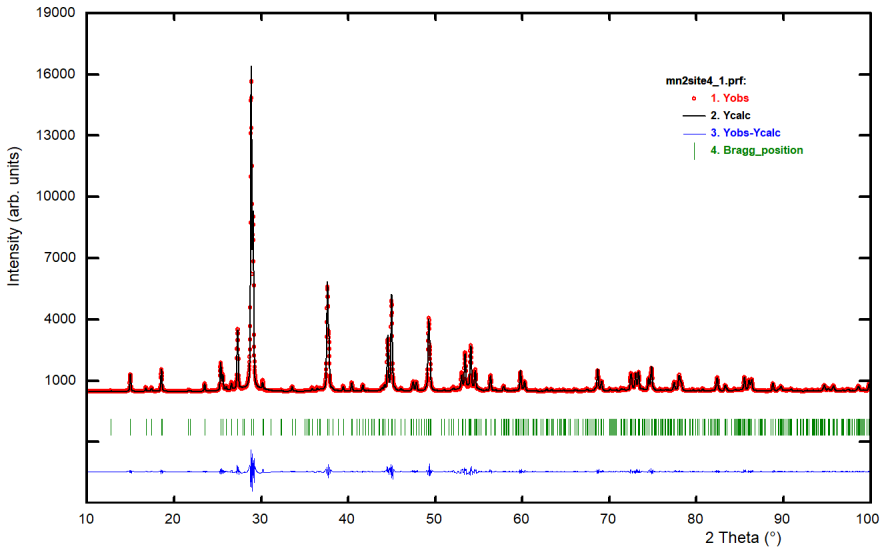

Table 3. Atomic coordinates, isotropic temperature factors, and interatomic distances for Mn_2SiTe_4.

Atom	Ox.	Site	*x*	*y*	*z*	foc	Biso (Å²)
Mn1	+2	4*a*	0	0	0	1	0.51(1)
Mn2	+2	4*c*	0.242(1)	¼	0.502(1)	1	0.51(1)
Si	+4	4*c*	0.406(1)	¼	0.073(1)	1	0.51(1)
Te1	-2	8*d*	0.328(1)	0.008(1)	0.252(1)	1	0.51(1)
Te2	-2	4*c*	0.415(2)	¼	0.687(2)	1	0.51(1)
Te3	-2	4*c*	0.585(2)	¼	0.245(1)	1	0.51(1)

Mn1-Te1^{ii}	2.89(1) x²	Mn1-Te2^{iii}	2.65(1) x²	Mn1-Te3^{iv}	2.88(1) x²
Mn2-Te1^{v}	2.83(1) x²	Mn2-Te1	2.82(1) x²	Mn2-Te2	2.69(3)
Mn2-Te3^{iii}	2.71(3)	--- --- ---	--- --- ---	--- --- ---	--- --- ---
Si-Te1	2.53(1) x²	Si-Te2^{i}	2.52(2)	Si-Te3	2.73(3)

Symmetry codes: (i) x, y, -1+z; (ii) -0.5+x, y, 0.5-z; (iii) -0.5+x, 0.5-y, 0.5-z; (iv) 0.5-x, -y, -0.5+z; (v) 0.5-x, -y, 0.5+z; (vi) x, 0.5-y, z.

chain below or above.

Each Mn_1Te_6 octahedron shares: 2 edges with 2 Mn_1Te_6 octahedra, 2 edges with 2 Mn_2Te_6 octahedra, 2 edges with 2 $SiTe_4$ tetrahedra; while each Mn_2Te_6 octahedron shares: 2 edges with 2 Mn_1Te_6 octahedra, 1 edge with 1 $SiTe_4$ tetrahedron. Figure 2 shows how the octahedra and tetrahedra share faces and corners.

The interatomic distances are shorter than the sum of the respective ionic radii for structures tetrahedrally bonded [42]. The Mn-Te bond distances, mean value 2.78(2) Å and Si-Te, mean value 2.59(2) Å are in good agreement with those found in the ICSD database [22], in the related compounds $MnIn_2Te_4$ [43], $Tl_2MnSnTe_4$ and $Tl_2MnGeTe_4$ [44], $Mn_3Si_2Te_6$ [45], $MnGa_2Te_4$ [46] and Ag_8SiTe_6 [47].

Figure 3 show the experimental magnetic susceptibility χ *versus* temperature T curve for the Mn2SiTe4 for 2 K < T < 300 K, and the corresponding inverse of susceptibility 1/ χ vs T curve. It is seen from Figure 3a) that in this range of temperature occur one transition at about 40 K.

The curve in Figure 2b is not a straight line, as in the ferromagnetic and antiferromagnetic cases. This result would indicate that below TN the ternary Mn_2SiTe_4 is not ferrimagnetic and instead it consists of anti-ferromagnetically couple planes of spins with a weak superimposed ferromagnetic component which can be attributed to spin canting. This behavior was also observed in Mn_2SiSe_4 [7]. The magnetic susceptibility measurement indicate a possible antiferromagnetic behavior for this material.

CONCLUSIONS

The crystal structure of the ternary compound Mn_2SiTe_4 was refined by the Rietveld method using X-ray powder diffraction data. This material was synthesized by direct fusion using the annealing method and crystallizes with an olivine-type structure in the orthorhombic space group *Pnma*.

Figure 2. Unit cell diagram of the new olivine-type compound Mn_2SiTe_4 (*Pnma*) showing the $MnTe_6$ octahedra and $SiTe_4$ tetrahedra sharing faces in the crystal structure.

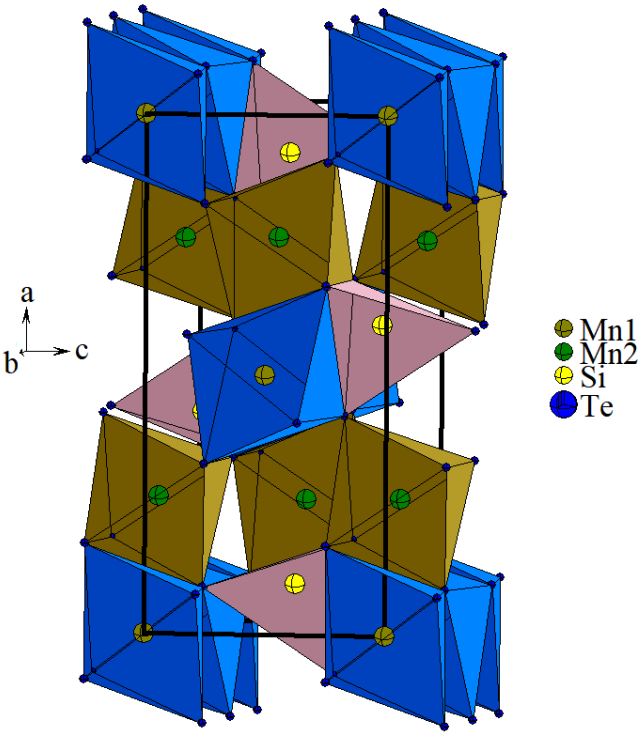

Figure 3. Variation of magnetic susceptibility $_{\chi}$ with T (a), and variation of $1/_{\chi}$ with T (b) for Mn_2SiTe_4.

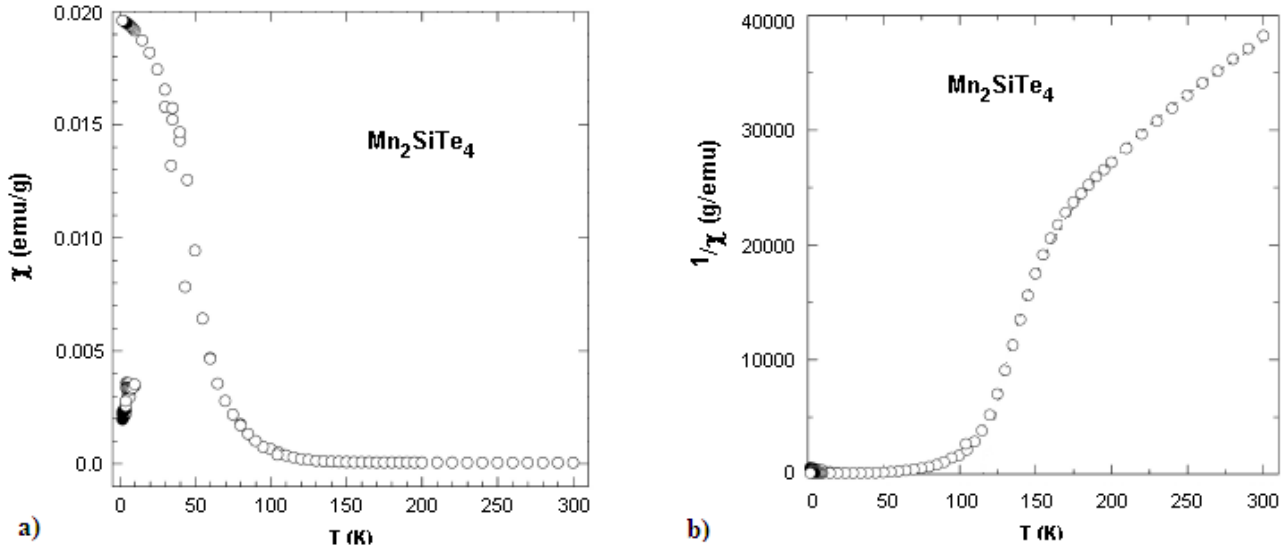

Its structure consists of a three-dimensional arrangement of lightly distorted $MnTe_6$ octahedra and $SiTe_4$ tetrahedra connected by common faces and corners and corresponds with a new compound of the II-III_2-VI_4 family with this crystalline arrangement. The magnetic susceptibility curve indicate a possible antiferromagnetic behavior for the Mn_2SiTe_4 compound.

ACKNOWLEDGEMENTS

This work was supported by CDCHT-ULA, and FONACIT Grant LAB-97000821.

REFERENCES

1. G. R. Desiraju, Cryst. *Growth Des.* 4, 896 (2011).
2. J. K. Furdyna, *J. Appl. Phys.* 64, R29-R64 (1988).
3. E. Parthé E. in *Intermetallic compounds, principles, and applications* edited by Westbrook J H & Fleischer R L (Jhon Wiley & Sons, New York), 1995.
4. J. C. Jumas, E. Philipot, M. Maurin, *Acta Cryst. B*, 33, 3850-3854 (1977).
5. M. Wintenberger, J. C. Jumas, *Acta Cryst B*, 36, 1993-1996 (1980).
6. W. L. Bragg, G. B. Brown, Z. Krist., 63, 538-556 (1926).
7. Fuhrmann, J. Pickardt, *Acta Cryst. C*, 45, 1808-1809 (1989).
8. S. Jobic, F. Bodenan, P. Le Boterf, G. Ouvrad, *J. Alloys Comp.* 230, 16-22 (1995).
9. M. Julien-Pouzol S. Jaulmes, S. Barnier, *J. Sol. Stat. Chem.* 65, 280-282 (1986).
10. H. J. Deiseroth, K. Aleksandrov, R. K. Kremer, Z. Anorg. A*llg. Chem.* 631, 448-450 (2005).
11. G. E. Delgado, L. Betancourt, A. J. Mora, J. E. Contreras, P. Grima-Gallardo, M. Quintero, *Av. Quím.* 4, 7-11 (2009).
12. C. Chacón, P. Delgado-Niño, G. E. Delgado, *Rev. Mex. Fís.* 66, 30-34 (2020).
13. G. E. Delgado, A. J. Mora, J. E. Contreras, L. Betancourt, *Bull. Mater. Sci.* 33, 247-249 (2010).
14. G. Lamarche, F. Lamarche, M. A. Lamarche, *Phys. B* 194-196, 219-220 (1993).
15. H. Mikus, H. J. Deiseroth, K. Aleksandrov, C. Ritter, R. K. Kremer, J. Inorg. Chem. 2007, 1515-1518 (2007).
16. V. K. Gudelli, V. Kanchana, G. Vaitheeswaran, *J. Phys. Cond. Matter.* 28, 025502(12) (2015).
17. A. Torres, D. E. Arroyo, M. E. Dompablo, *J. Phys. Chem. C* 122, 9356-9362 (2018).
18. A. Junod, K. O. Wang, G. Triscone, G. Lamarche, *J. Magn. Magn. Mater.* 146, 21-29 (1995).
19. M. Quintero, D. Ferrer, D. Caldera, E. Moreno, E. Quintero, M. Morocoima, P. Grima, P. Bocaranda, G. E. Delgado, J. A. Henao, *J. Alloys Compd.* 469 4-8 (2009).
20. M. Partik, T. H. Sting, H. D. Lutz, H. Sabrowsky, P. Z. Vogt, Z. Anorg. *Allg. Chem.* 621, 1600-1604 (1995).
21. R. C. Haushalter, C. J. O'Connor, A. M. Umarji, G. K. Shenoy, C. K. Saw, Solid State Comm. 49, 929-933 (1984).
22. ICDD-International Centre for Diffraction Data, Powder Diffraction File (Set 1-69). Newtown Square, USA, 2017.
23. ICSD-Inorganic Crystal Structure Database, Gemlin Institute, Kalrsruhe, Germany, 2016.
24. SpringerMaterials, *https://materials.springer.com.*
25. X. Zhang, V. Stavanovic, M. Davezac, S. Lany, A. Zunger, *Phys. Rev. B* 86, 014109 (14) (2012).
26. L. M. Martinez, H. Iturriaga, R. Olmos, L. Shao, Y. Liu, T. Mai, C. Petrovic, A. R. Hight, S. R. Singamaneni, *J. Appl. Phys.*

Lett. 116, 172404(5) (2020).
27. J. H. Yang, J. H. Ang, H. Xiang, *Nature Mater.* 18 1273-1274 (2019).
28. G. E. Delgado, E. Quintero, R. Tovar, P. Grima, M. Quintero, *J. Alloys Comp.* 613 143-145 (2014).
29. G. E. Delgado, A. J. Mora, P. Grima, M. Muñoz, S. Durán, M. Quintero, J. M. Briceño, Bull. *Mater. Sci.* 38,1061-1064 (2015).
30. C. Rincón, G. Marcano, R. Casanova, G. E. Delgado, G. Marin, G. Pérez-Sánchez, *phys. stat. sol.* (b) 253, 697-704 (2016).
31. G. E. Delgado, P. Grima-Gallardo, L. Nieves, H. Cabrera, J. R. Glenn, J. A. Aitken, *Mater. Res.* 19, 1423-1428 (2016).
32. G. E. Delgado, J. A. Flores, P. Grima-Gallardo, M. Quintero, A. Moreno, *Mater. Res.* 29, e20160748 (2018).
33. G. E. Delgado, L. Manfredy, S. A. López-Rivera, *Powder Diffr.* 33, 237-241 (2018).
34. C. Rincón, E. Quintero, M. Quintero, E. Moreno, C. Power, M. Morocoima, G. E. Delgado, *phys. stat. sol.* (b) 256, 1900076(8) (2019).
35. G. E. Delgado, P. Delgado-Niño, P. Grima-Gallardo, *Period. Tchê Quím.* 16, 848-853 (2019).
36. G. E. Delgado, G. Guedez, G. Sánchez-Pérez, C. Rincón, G. Marroquin, *Rev. Matéria 24*, e1232900(5) (2019).
37. M. Solzi, C. Pernechele, G. Attolini, G. E. Delgado, V. Sagredo, J. Magn. Magn. Mater. 498, 166164(7). (2020)
38. A. Boultif, D. Louer, *J. Appl. Cryst.* 37, 724-731 (2004).
39. H. M. Rietveld, J. Appl. Cryst. 2, 65-71 (1969).
40. J. Rodríguez-Carvajal, Fullprof, version 7.4, LLB, CEA-CNRS, France, March 2023.
40. G. Cagliotti, A. Paoletti, P. Ricci, Nucl. Instr. 3, 223-228 (1958).
41. P. Thompson, D. E. Cox, J. B. Hastings, *J. Appl. Cryst*. 20, 79-83 (1987).
42. R. D. Shannon, *Acta Cryst. A*, 32, 751-767 (1976).
43. G. E. Delgado, C. Chacón, J. M. Delgado, V. Sagredo, *phys. stat. sol*. (a) 134, 61-66 (1992).
44. M. A. McGuire, T. J. Scheidemantel, J. V. Badding, F. J. DiSalvo, *Chem. Mater.* 17, 6186-6191 (2005).
45. H. Vincent, D. Leroux, D. Bijaoui, R. Rimet, C. Schlenker, *J. Solid. State Chem.* 63, 349-352 (1986).
46. M. Cannas, A. Garbato, L. Garbato, F. Ledda, G. Navarra, Prog. Cryst. Growth Charact. *Mater.* 32, 171-183 (1996).
47. F. Boucher, M. Evain, R. Brec, *J. Solid State Chem.* 100, 341-355 (1992).